Ex-Situ Development and Characterization of Composite Film Based on Bacterial Cellulose Derived from Oil Palm Frond Juice and Chitosan as Food Packaging

Norshafira Syazwani Abu Hasan[1], Shahril Mohamad[1], Sharifah Fathiyah Sy Mohamad[1]*, Mohd Hafiz Arzmi[2,3] and Nurul Nadia Izzati Supian[1]

[1]*Faculty of Chemical of Process Engineering Technology, College of Engineering Technology, Universiti Malaysia Pahang, 26300 UMP, Kuantan, Pahang, Malaysia*
[2]*Department of Fundamental Dental and Medical Sciences, Kulliyyah of Dentistry, International Islamic University Malaysia, 25200 IIUM, Kuantan Campus, Pahang, Malaysia*
[3]*Cluster of Cancer Research Initiative IIUM (COCRII), International Islamic University Malaysia, 25200 IIUM, Kuantan, Pahang, Malaysia*

ABSTRACT

The development of alternative food packaging films using bio-based residues is in great demand for replacing petroleum-based packaging materials. However, large-scale application is severely limited by costly production and poor performance. This study investigates the ex-situ modification of bacterial cellulose (BC) produced by *Acetobacter xylinum* in oil palm fronds juice to obtain BC-Chitosan (BCC) films. FTIR revealed the structure of amide I and II bands, confirming the presence of chitosan in BCC films. The FE-SEM images of BCC films showed the formation of a thick chitosan layer with increasing chitosan incorporated into the BC surface structure. The coated chitosan layer observed improved mechanical properties in BCC films due to the disappearance of empty pores between BC fibers. Increments in chitosan concentration slightly decreased the thermal behavior of BCC. The antimicrobial effects of BCC films were effective against Gram-positive bacteria (*Staphylococcus aureus*) when the concentration of chitosan incorporated was above 0.6 %w/v. This study reveals the potential of extending the application of BC derived from oil palm frond juice (OPFJ) for developing food packaging materials.

Keywords: Bacterial cellulose, chitosan, *ex-situ* method, film composite, oil palm frond juice

INTRODUCTION

High consumption of non-biodegradable food packaging materials derived from petroleum-based polymers has raised environmental concerns. As a result, there is an increased interest in designing new packaging materials derived from renewable or natural sources as green alternatives for controlling the environmental impacts of the massive use of conventional plastic packaging (Oliveira et al., 2020). In this sense, bacterial cellulose (BC), produced by an inexpensive approach, can act as a base material in developing biodegradable packaging. BC is a biodegradable polymer commonly synthesized by *Acetobacter xylinum,* a widely used bacteria, due to its ability to change the sugar mixture into cellulose under specific conditions (Kongruang, 2007). In addition, BC is known to exhibit various unique properties, such as high cellulose purity, high water-holding capacity, biocompatibility, and biodegradability (Bandyopadhyay et al., 2018). Therefore, BC has found promising potential to be considered as an alternative biopolymer in medical, paper, and food applications (Azeredo et al., 2019). However, large-scale application of BC suffers from low yield as well as high cost of production due to the highly-priced Hestrin-Schramm media used in conventional BC cultivation (Lin et al., 2020). These drawbacks led to the exploration of alternative culture mediums derived from either agricultural wastes or industrial byproducts to minimize the production cost of BC.

Recently, several studies have shown the use of low-cost alternative culture media such as orange-peel wastes (Kuo et al., 2019), acerola byproducts (Leonarski et al., 2021), and wheat thin stillage (Revin et al., 2018) to produce BC. The utilization of these wastes has proven to enhance the BC yield and reduce the production cost of BC due to the abundant availability of the wastes (Hussain et al., 2019; Revin et al., 2018). The Malaysian oil palm industries produce a large quantity of oil palm biomass consisting of oil palm fronds, empty fruit bunches, oil palm trunks, palm kernel shells, mesocarp fibers, and palm oil mill effluent. The oil palm fronds, the outcome of pruning and harvesting palm oil trees, contribute to 75% of the solid wastes, at approximately 83 million tons annually (Yusof et al., 2019). The basal part of the oil palm frond (OPF) petiole can be squeezed to obtain fresh oil palm frond juice (OPFJ). The OPFJ contains a high quantity of fermentable sugars (up to 40 g/L of glucose, sucrose, and fructose), minerals, and nutrients (Zahari et al., 2012). The abundant availability of OPF all year round and the large sugars and nutrient contents of OPFJ rendered it a suitable fermentation medium. OPFJ-based culture medium was recently utilized in the fermentation of bioethanol, biobutanol, succinic acid, and poly(3-hydroxybutyrate). In addition, previous research has demonstrated the potential of producing BC using OPFJ as the only culture medium without any other nutrients or supplementation needed (Supian et al., 2021). Thus, replacing the expensive HS conventional medium with the alternative culture medium derived from OPFJ is a promising method to produce BC with minimum production cost.

BC produced from agricultural wastes could be an excellent biomaterial choice for bio-based film food packaging development. However, many issues need to be addressed before BC's unlimited potential as a choice of material can be completely realized. For example, BC films alone have low mechanical properties and poor antimicrobial resistance, hindering the broader commercialization potential of BC-based packaging material. Hence, many strategies were proposed to overcome these weaknesses, including impregnating BC with another polymer, such as chitosan. Chitosan is another natural material with antimicrobial activity, which is relatively low in cost and has abundant availability. As a food packaging material, incorporating BC film with chitosan should prevent microbial growth on the food surface by controlling the foodborne pathogenic bacteria, improving the mechanical properties, and reducing the cost (Malhotra et al., 2015).

There have been numerous studies on the development of BC-based films made from BC and chitosan. However, most studies focused on developing BC-Chitosan composites for biomedical applications and using BC produced from the commercial Hestrin-Schramm medium. However, to our knowledge, the combined effects of BC derived from the OPFJ with chitosan have never been explored. Therefore, in this study, the OPFJ was employed as the culture medium to produce BC by static cultivation of *Acetobacter xylinum*. The BC-produced synthesized BC-Chitosan (BCC) films with 0.2, 0.6, and 1.0% w/v chitosan by direct immersion into the chitosan solutions. All samples were characterized based on their chemical, morphological, mechanical, thermal, and antimicrobial properties for potential application as food packaging materials. These findings elucidate BCC films as a promising alternative for various packaging applications.

MATERIALS AND METHODS

Materials

Fresh oil palm frond was collected from LKPP Oil Palm Plantation in Pekan, Pahang, Malaysia. Chitosan of medium molecular weight, sodium hydroxide, acetic acid, microcrystalline cellulose (MCC), and α-cellulose were procured from Sigma-Aldrich. *Acetobacter xylinum* FTCC 0416 was supplied by the Malaysian Agriculture Research and Development Institute (MARDI), Serdang, Selangor, Malaysia. All other chemicals and reagents used were of the analytical grade.

Production and Purification of BC

OPFJ feedstock was extracted from OPF petioles harvested a day earlier to maintain freshness. Fresh OPFJ was obtained by pressing the OPF petiole with a hydraulic pressing machine (MATSUO Inc., Japan). Impurities contained in the extracted OPFJ were removed using a 0.5 mm stainless steel sieve followed by a muslin filter cloth. The filtered OPFJ was centrifuged (10000 rpm, 4ºC, 20 min) and kept at -20ºC before use. BC was produced

using 80% v/v OPFJ (adjusted to pH 4.5) as the culture medium. The medium was inoculated with 10% v/v *A. xylinum* and statically incubated for 14 days at 30ºC. The BC pellicles formed at the top of the culture medium were harvested at the end of 14 days and repeatedly washed using distilled water. The BC pellicles were then purified by boiling them in 0.5 M NaOH for 2 h to ensure that the BC surface was free from bacterial cell attachment. Finally, the pure BC pellicles were washed with distilled water several times until a neutral pH was attained.

Preparation of BC-Chitosan (BCC) Composite Films

The BCC composites were prepared following the method of Kim et al. (2011) with slight changes. Three different concentrations of chitosan solutions (0.2, 0.6, and 1.0% w/v) were prepared by dissolving chitosan powder in 1% v/v acetic acid at room temperature for 2 h. Preparation of BC-Chitosan (BCC) films was carried out by first positioning the neutralized BC pellicles between two filter paper sheets to absorb excessive water. The BC was then immersed in 50 ml chitosan solution for 24 h at 50ºC. Finally, the BCC films were removed from the solution, washed with deionized water, placed between two filter paper sheets to remove the excess solution, and weighed before being pressed with an iron to form dried BCC films. The samples were labeled as BC (without chitosan), BCC-0.1, BCC-0.6, and BCC-1.0 corresponding to the chitosan concentrations used (% w/v).

Characterization of BC and BCC Films

Chemical Structure by Attenuated Total Reflection Fourier-Transform Infrared (ATR-FTIR) Spectroscopy. The chemical structure of BC and BCC films was analyzed using an FTIR spectrophotometer (Nicolet iS5, Thermo Fisher Scientific, USA) with an attenuated total reflectance (ATR) mode. For each sample, 32 scans with a resolution of 4 cm^{-1} were collected over the wavenumber ranging from 400–4000 cm^{-1} in transmittance mode.

Surface Morphology by Field Emission Scanning Electron Microscopy (FE-SEM). The pure BC and BCC films' surface morphology was visualized with a DSM 940A high-resolution Field Emission Scanning Electron Microscope (FE-SEM; Zeiss, Germany) operated at 15 kV.

Mechanical Properties. The mechanical properties of the BC and BCC films were determined using a texture analyzer machine (CT3 Texture Analyzer, Brookfield, USA) equipped with TexturePro CT V1-8 Build 3.1. The samples were prepared by cutting each BC and BCC film into strips (70 mm x 10 mm) using a precise cutter. Tensile strength (TS), percentage of elongation at break (%EAB), and Young's Modulus (YM) were measured according to the standard method D-882 (ASTM, 2002). An initial grip separator of about 50 mm and a 50 mm/min of crosshead speed was used to run the tests. In every test, TS and %EAB were computed using Equations 1 and 2, respectively (Cazón et al., 2019).

$$TS(MPa) = \frac{F}{A} \qquad\qquad [1]$$

$$\%EAB = \frac{L}{60} \times 100 \qquad\qquad [2]$$

In Equation 1, F is the maximum load that is required in pulling apart the sample (N), and A is the cross-sectional area (m^2). Meanwhile, in Equation 2, L is the film elongation during the rupture (mm), and 60 is the initial length of grip (mm) of the film samples. Young's modulus was computed from the initial stress-strain curve slope, expressed in MPa.

Thermal Properties Using Thermogravimetric Analysis (TGA). TGA was carried out on all BC and BCC samples to evaluate their respective mass losses when subjected to continuous heating. TGA was performed using TGA Instrument Q500 V 6.7 (TA Instruments, USA) with a 10°C/min heating rate from 25 to 800°C under a nitrogen atmosphere.

Antimicrobial Susceptibility Testing. The antimicrobial susceptibility of pure BC and BCC films was carried out according to the Kirby-Bauer disc diffusion method. *Candida albicans* ATCC (MYA-4901), *Staphylococcus aureus* (ATCC 25923), and *Escherichia coli* (ATCC 25922) were selected as the representative of yeast, Gram-positive bacteria, and Gram-negative bacteria in the antimicrobial susceptibility tests. The stock culture was revived by inoculating the yeast and the bacteria into yeast peptone dextrose (YPD) and brain heart infusion (BHI) broth, respectively, and incubated at 37ºC overnight. Briefly, two yeast and bacteria colonies were inoculated into 5 ml of the nutrient broth. Subsequently, the inoculum was standardized to 0.5 McFarland standard, which equals OD600 nm 0.1. 100 µL of the yeast and bacteria suspension were inoculated into a nutrient agar (Oxoid, UK) plate using a sterile cotton swab. Samples of BC (control group) and BCC films priorly to sterilization were then placed onto the surface of the agar medium and incubated at 37ºC for 24 h. The inhibition zone was estimated by measuring the bacterial growth inhibition zone diameter around the samples. The diffusion assay was performed in triplicate.

RESULTS AND DISCUSSION

Characterization of BC and BCC Films

ATR-FTIR Spectroscopy Analysis. ATR-FTIR spectroscopy was performed to identify the functional groups of BC and evaluate the structural interaction between BC and chitosan due to the incorporation of different concentrations of chitosan (0.2–1.0% w/v) into the

BC film matrix by measuring the spectra in the wavenumber range of 4000-400 cm^{-1} at a spectral resolution of 4 cm^{-1}. The FTIR spectra of BC, MCC, and α-cellulose were analyzed to have a comparative view of the functional groups in cellulose. As shown in Figure 1, the BC obtained in this study showed all the typical characteristic peaks of cellulose, similar to MCC and α-cellulose, indicating that the BC had a cellulose structure. The peaks observed at 3340 cm^{-1} and 2893 cm^{-1} correspond to the stretching vibrations of the O-H groups of cellulose and the C-H stretching, respectively (Ju et al., 2020). The peak at 1630 cm^{-1} corresponds to the glucose carbonyl group (C=O) (He et al., 2020). Meanwhile, the band at 1427 cm^{-1} is from CH_2 symmetric bending, and the band at 1369 corresponds to the C-H deformation vibration. Furthermore, the peaks observed at 1161 cm^{-1} and 1107 cm^{-1} indicated the C-O-C deformation vibration and C-C bending, respectively. Finally, the peaks at 897 cm^{-1} are from the β-glycosidic linkages in the cellulose structure.

Figure 2 compares FTIR spectra between the BC and BCC films containing different chitosan amounts. The obtained spectra revealed that the prominent characteristic peaks of BC are still observed in the BCC films. The broad bands between 3300 cm^{-1} and 3278 cm^{-1} in all the samples indicated the O-H and N-H stretching vibrations. Meanwhile, the symmetric and asymmetric C-H stretching vibrations lead to peaks around 2918 cm^{-1} and 2893 cm^{-1}. Moreover, the bands at 1636 and 1541 cm^{-1} are attributed to C=O stretching (amide I) and N-H bending (amide II), respectively. Finally, the bands located between 1028-1030 cm^{-1} correspond to the stretching vibrations of C-O.

Both BC and chitosan have similar chemical compositions. Thus, the appearance of the amide groups on the IR spectra corroborated the presence of chitosan within the BCC film. IR spectra are proven useful in verifying the existence of chitosan molecules in BCC film (Lin et al., 2013). In this study, the band corresponding to the amide III could only be observed in the BCC-1.0 sample. The low peak intensity could be correlated because the chitosan signal has a lower concentration than the more vigorous BC peak intensity. The low availability of chitosan in the BCC film might also contribute to the low-intensity peak at 1371 cm^{-1} (amide III). On the other hand, higher intensity of the broad peak corresponding to the hydrogen bond absorption band was observed in pure BC than in the BCC films. It might be due to the hydrogen bonds' partial break between the BC hydroxyl groups, which is caused by the penetration of chitosan into the structure of BC (Ju et al., 2020). The decreasing and slight shift of the absorption band in the composite corresponding to Iα crystalline cellulose allomorph might indicate a disruption of BC crystallinity in the presence of chitosan interfering with BC intermolecular hydrogen bonds. Similar findings were also observed in other studies of BC/chitosan composites (Jia et al., 2017).
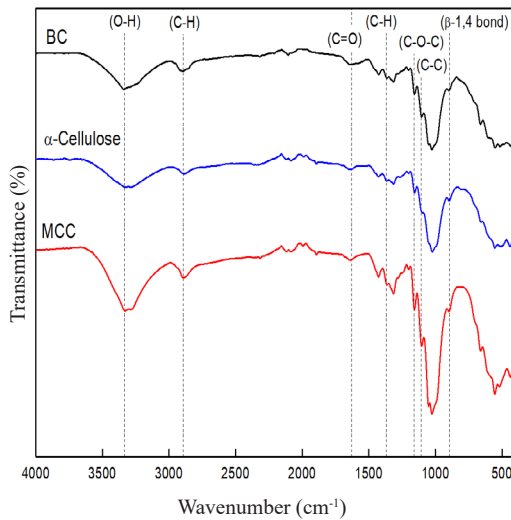
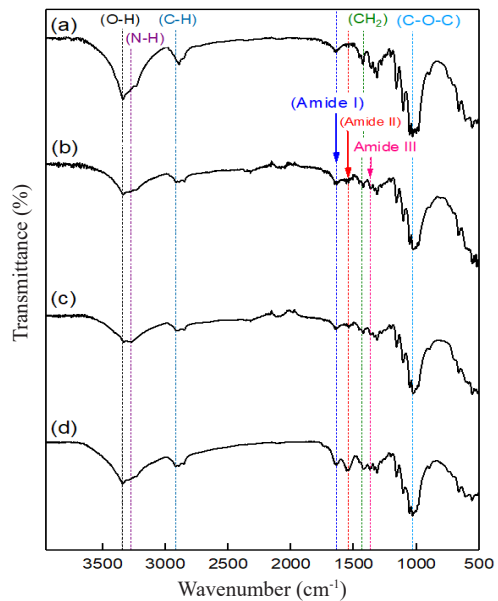Figure 1. FTIR spectra of BC obtained from OPFJ, MCC, and α-Cellulose

Figure 2. FTIR spectra of (a) pure BC and BCC films prepared using (b) 0.2% w/v, (c) 0.6% w/v, and (d) 1.0% w/v chitosan

Surface Morphology of BC and BCC Films. FE-SEM analysis was used to evaluate the surface morphology of the BC and BCC films and verify the degree of penetration of chitosan inside the BC. Figure 3 presents the surface morphology of each BC and BCC film examined by the FE-SEM. Figure 3a revealed that the pure BC film showed a densely packed, interwoven, connected, and randomly oriented network of fibers, with fiber diameters that range from 28 to 62 nm. The observation agrees with the morphology reported for BC produced statistically in alternative media (Dubey et al., 2017; Sharma et al., 2021). Moreover, a further increase of chitosan concentration in BCC films (Figures 3b-d) resulted in forming of a thick and coarse layer, probably due to the disappearance of the porous structure into the BC matrix that filled the gap between the adjoining BC fibers. These results implied that chitosan might penetrate within the BC microfibrils, leading to a more compact network structure with less pore size (Ul-Islam et al., 2011). Several studies also reported similar findings in the changes of the physicochemical properties with the increment of chitosan content incorporated in the BC films (Kim et al., 2011; Tanpichai et al., 2020).

Mechanical Properties. The mechanical properties of BC and BCC films were evaluated to estimate the quality of packaging materials, and the results are shown in Figure 4. In this study, the tensile strength increased with increasing chitosan concentration. Meanwhile, the elongation at break of the BC first decreased with increasing chitosan concentration and then increased when 1.0% w/v chitosan was used. In contrast, Young's modulus increased when chitosan concentration increased, reaching a maximum of BCC-0.6, then decreasing

to 1360 MPa (BCC-1.0). All these findings suggested that the BCC composites were more resilient with increasing concentrations of chitosan used.
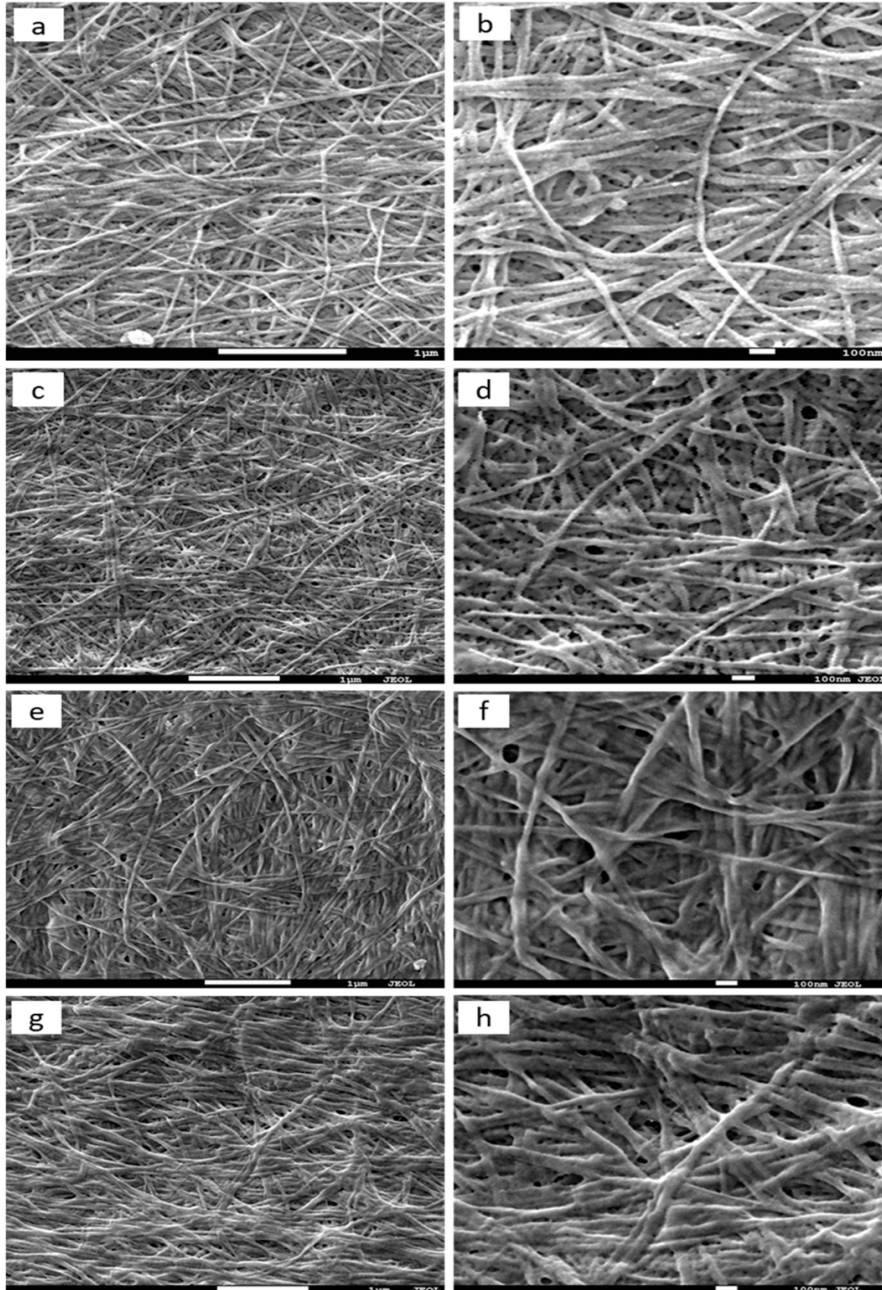

Figure 3. FE-SEM images of (a) BC ×25,000; (b) BC ×50,000; (c) BCC-0.2 ×20,000; (d) BCC-0.2 ×50,000; (e) BCC-0.6 ×25,000; (f) BCC-0.6 ×50,000; (g) BCC-1.0 ×20,000 and (h) BCC-1.0 ×50,000 magnifications
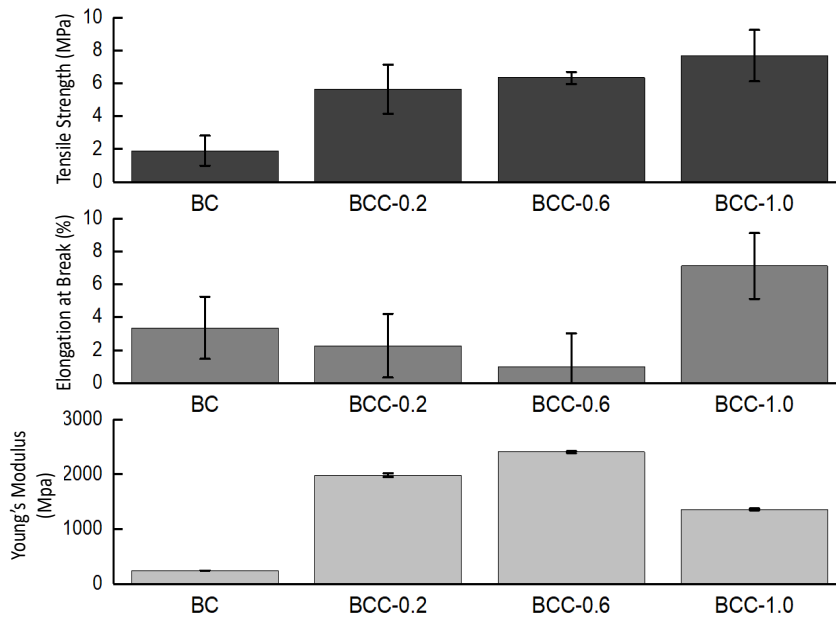
Figure 4. Tensile strength, elongation at break, and Young's modulus of BC and BCC films

The BCC films developed in this study demonstrated higher mechanical properties (tensile strength and elastic modulus) than pure BC film, indicating that the BCC could be a suitable alternative food packaging material. These results may correspond to the intermolecular hydrogen bond formation between the chemical groups in bacterial cellulose (–OH) and chitosan (–OH and –NH2), which hinders the matrix mobility while enhancing its rigidity (Liang et al., 2019). Also, we found that the BC produced from OPFJ cultivation displayed considerably high mechanical properties than the ones reported by Lin et al. (2013). The differences in mechanical properties could be due to culture time, medium supplements, or post-treatment variations for the BC (Sharma et al., 2021). Nevertheless, the elongation at the break of our BCC films was lower, contrasting with that of other BCC composites reported by Lin et al. (2013). The low elongation at break might be attributed to the brittle structure of the dried BCC films with increasing chitosan concentrations.

Thermal Properties by TGA. The thermal characteristics of BC and BCC films were tested using TGA, and the TG curves of each tested BC and BCC film as a function of temperature is presented in Figure 5. For all samples, three stages of weight loss were observed in the TGA curves. The initial stage of weight loss at 50–150°C was ascribed to the evaporation of the retained moisture in both BC and BCC samples (Du et al., 2018). The water volatilization led to a weight loss of 7.90, 9.33, 12.50, and 14.31% for samples

from BC, BCC-0.2, BCC-0.6, and BCC-1.0, respectively. The weight loss percentage until 150°C increased when chitosan concentration increased because of its hydrophilic nature. The increment of weight loss percentages observed in BCC samples might be associated with the condensation of water molecules on its surface due to the hygroscopicity character of the chitosan that retained the adsorbed moisture strongly at standard relative humidity conditions (Cazón et al., 2019).

For all BC and BCC samples, major weight losses were observed in the second stage at 200-350°C attributed to the thermal decomposition of the rapid cleavage of BC glycosidic bond and chitosan (Wahid et al., 2019). At 350°C, the total weight loss values were 85.93, 66.91, 64.11, and 66.75% for BC, BCC-0.2, BCC-0.6, and BCC-1.0 samples, respectively. The weight loss decreases as the BCC's chitosan concentration increases and becomes saturated after 0.6% w/v of chitosan concentration.
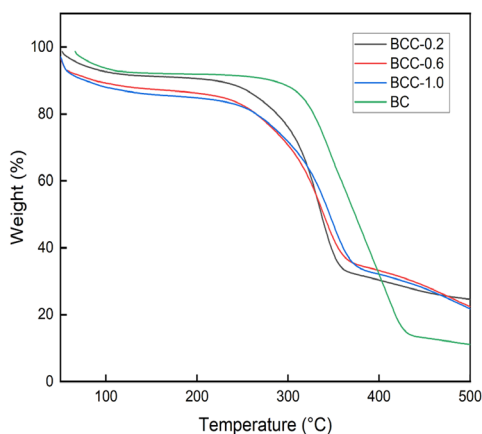

Figure 5. TGA curves of BC and BCC samples

Prior research shows BC's maximum thermal degradation temperature was 330°C (Cacicedo et al., 2020). In this study, the maximum thermal degradation temperature for BC derived from OPFJ was 342°C. The addition of chitosan to the BC matrix slightly shifted the maximum thermal degradation temperature from 342°C (BC) to 335°C (BCC-0.2), 338°C (BCC-0.6), and 328°C (BCC-1.0), indicating the presence of intermolecular interaction between BC and chitosan. However, BCC samples' thermal stability is reduced compared to BC. Similar TGA results were obtained by Jia et al. (2017). The reduced thermal stability of BCC samples could probably be due to the weaker interfacial hydrogen bonding between BC and chitosan. In addition, the thermal stability of BCC is also known to depend on these various intrinsic (degree of deacetylation, molecular weight, and purity of chitosan) and extrinsic (storage conditions and thermal processing method) factors (Szymańska & Winnicka, 2015).

The third weight loss region ranging from 360 to 500°C, was associated with the final decomposition of the vestigial carbon of BC to ash. When the heating process was almost completed, the total weight loss values were 88.86, 75.32%, 77.25, and 78.12% for BC, BCC-0.2, BCC-0.6, and BCC-1.0, respectively. The lower weight losses observed in all BCC samples implied that the BCC composites decomposed slower than BC. Nevertheless, the outcomes of thermal stability showed that the BCC composite films developed are stable at temperatures below 150°C. Therefore, this biodegradable blend material is more likely to be applied to food products post-sterilization or pasteurization.

Antimicrobial Susceptibility Testing. In the current work, since chitosan possesses antimicrobial properties, we hypothesized that the BCC films would demonstrate a similar action to the BC control film. Figure 6 presents the antimicrobial effect of BC and BCC films against Gram-positive (*S. aureus*) and Gram-negative (*E. coli*) bacteria and the antifungal activity against *C. albicans*. As expected, the BC film samples showed no antimicrobial activity against the three selected microorganisms. Interestingly, all BCC films (BCC-0.2, BCC-0.6, and BCC-1.0) also showed no inhibition of *E. coli* or *C. albicans.* The findings showed that the chitosan could be tightly incorporated in BC fibrils, preventing the diffusion of the antimicrobial component from BCC films to the surrounding agar to create the inhibition zone (Lin et al., 2013). While several authors reported significant improvement in the antimicrobial properties of BCC against Gram-positive and Gram-negative bacteria, the present results were in accordance with several studies which show the absence of antimicrobial properties of chitosan against tested microorganisms when fabricated in the solid form (Lin et al., 2013).

This study, however, demonstrated that the inhibition zone was only observed against the Gram-positive *S. aureus* for BCC-0.6 and BCC-1.0, with an inhibition zone diameter of 30.66 ± 0.28 and 32.48 ± 0.51 mm, respectively. The findings indicate that the antimicrobial activity of the BCC film was more effective against *S. aureus* than *E. coli* and *C. albicans*. The different thicknesses of the bacterial peptidoglycan layers might contribute to the high sensitivity of chitosan in BCC films against the Gram-positive *S. aureus*. By contrast, the peptidoglycan layer of Gram-positive bacteria (7–8 nm) is thinner than Gram-negative bacteria (20–80 nm). The finding also suggested that a minimum concentration of 0.6% w/v chitosan is sufficient to act as an antimicrobial agent against *S. aureus*. On the other hand, insufficient chitosan incorporated in the BCC film and the slow migration of chitosan from the BCC film matrix might be the reasons for the lack of antimicrobial activity observed for the BCC-0.2 sample (Dehnad et al., 2014).

The difference in the antimicrobial effects of chitosan was probably due to the variations in the antimicrobial mode of action and the disparities in the composition and structure of the cell walls of the three selected microorganisms (Buruaga-Ramiro et al., 2020). Although the exact antibacterial mechanism of chitosan remains unclear, several theories proposed that the antimicrobial mechanism of chitosan was probably due to the suppression of the generation of mRNA bacterial cells triggered by the electrostatic interactions between the positively charged amino groups (NH_3^+) in chitosan molecules and the anionic teichoic acids in the bacterial cell wall. As a result, the permeability of the bacteria cell membrane will also increase and causing the inhibition of cell growth (Liang et al., 2019; Wahid et al., 2019).
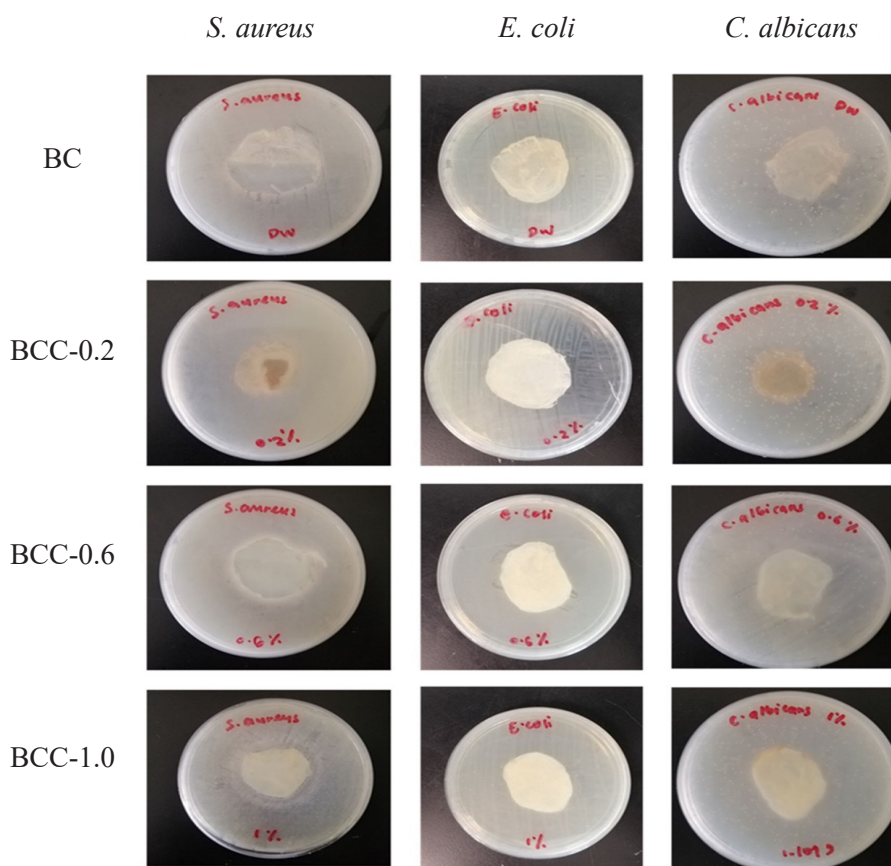
Figure 6. Disk diffusion results of BC and BCC films against three different microbes

CONCLUSION

The present study successfully produced BCC film composites to reduce the environmental harm caused by synthetic plastic packaging materials. BCC films were prepared via the *ex-situ* method involving immersion of BC derived from the static cultivation of *A. xylinum* in OPFJ in various concentrations of chitosan solution. The ATR-FTIR and FE-SEM results confirm the successful incorporation of chitosan into the BC. The BCC films also displayed enhanced mechanical properties compared to BC alone. Meanwhile, the antimicrobial properties of chitosan remained in the BCC-0.6 and BCC-1.0 against the Gram-positive *S. aureus*. The thermal behavior of the BCC films suggested the possibility of being applied in foods that are heat-treated until 150°C. Hence, BCC films from BC produced through OPFJ cultivation can offer a suitable innovative replacement for non-biodegradable food packaging materials. Further study on the effect of plasticizer type and content is recommended to obtain excellent mechanical properties, as demonstrated by commercial plastic-based materials.

ACKNOWLEDGEMENTS

REFERENCES

Azeredo, H. M. C., Barud, H., Farinas, C. S., Vasconcellos, V. M., & Claro, A. M. (2019). Bacterial cellulose as a raw material for food and food packaging applications. *Frontiers in Sustainable Food Systems*, *3*, 1-14. https://doi.org/10.3389/fsufs.2019.00007

Bandyopadhyay, S., Saha, N., Brodnjak, U. V., & Saha, P. (2018). Bacterial cellulose based greener packaging material: A bioadhesive polymeric film. *Materials Research Express*, *5*(11), Article 115405. https://doi.org/10.1088/2053-1591/aadb01

Buruaga-Ramiro, C., Valenzuela, S. V., Valls, C., Roncero, M. B., Pastor, F. I. J., Díaz, P., & Martinez, J. (2020). Development of an antimicrobial bioactive paper made from bacterial cellulose. *International Journal of Biological Macromolecules*, *158*, 587-594. https://doi.org/10.1016/j.ijbiomac.2020.04.234

Cacicedo, M. L., Pacheco, G., Islan, G. A., Alvarez, V. A., Barud, H. S., & Castro, G. R. (2020). Chitosan-bacterial cellulose patch of ciprofloxacin for wound dressing: Preparation and characterization studies. *International Journal of Biological Macromolecules*, *147*, 1136-1145. https://doi.org/10.1016/j.ijbiomac.2019.10.082

Cazón, P., Velázquez, G., & Vázquez, M. (2019). Characterization of bacterial cellulose films combined with chitosan and polyvinyl alcohol: Evaluation of mechanical and barrier properties. *Carbohydrate Polymers*, *216*, 72-85.

Dehnad, D., Mirzaei, H., Emam-Djomeh, Z., Jafari, S. M., & Dadashi, S. (2014). Thermal and antimicrobial properties of chitosan-nanocellulose films for extending shelf life of ground meat. *Carbohydrate Polymers*, *109*, 148-154. https://doi.org/10.1016/j.carbpol.2014.03.063

Du, R., Zhao, F., Peng, Q., Zhou, Z., & Han, Y. (2018). Production and characterization of bacterial cellulose produced by gluconacetobacter xylinus isolated from Chinese persimmon vinegar. *Carbohydrate Polymers*, *194*, 200-207. https://doi.org/10.1016/j.carbpol.2018.04.041

Dubey, S., Sharma, R. K., Agarwal, P., Singh, J., Sinha, N., & Singh, R. P. (2017). From rotten grapes to industrial exploitation: Komagataeibacter europaeus SGP37, a micro-factory for macroscale production of bacterial nanocellulose. *International Journal of Biological Macromolecules*, *96*, 52-60. https://doi.org/10.1016/j.ijbiomac.2016.12.016

He, F., Yang, H., Zeng, L., Hu, H., & Hu, C. (2020). Production and characterization of bacterial cellulose obtained by Gluconacetobacter xylinus utilizing the by-products from Baijiu production. *Bioprocess and Biosystems Engineering*, *43*, 927-936. https://doi.org/10.1007/s00449-020-02289-6

Hussain, Z., Sajjad, W., Khan, T., & Wahid, F. (2019). Production of bacterial cellulose from industrial wastes: A review. *Cellulose*, *26*, 2895-2911. https://doi.org/10.1007/s10570-019-02307-1

Jia, Y., Wang, X., Huo, M., Zhai, X., Li, F., & Zhong, C. (2017). Preparation and characterization of a novel bacterial cellulose/chitosan bio-hydrogel. *Nanomaterials and Nanotechnology*, *7*, 1-8. https://doi.org/10.1177/1847980417707172

Ju, S., Zhang, F., Duan, J., & Jiang, J. (2020). Characterization of bacterial cellulose composite films incorporated with bulk chitosan and chitosan nanoparticles: A comparative study. *Carbohydrate Polymers*, *237*, Article 116167. https://doi.org/10.1016/j.carbpol.2020.116167

Kim, J., Cai, Z., Lee, H. S., Choi, G. S., Lee, D. H., & Jo, C. (2011). Preparation and characterization of a bacterial cellulose/chitosan composite for potential biomedical application. *Journal of Polymer Research*, *18*, 739-744. https://doi.org/10.1007/s10965-010-9470-9

Kongruang, S. (2007). Bacterial cellulose production by acetobacter xylinum strains from agricultural waste products. In W. S. Adney, J. D. McMillan, J. Mielenz, K. T. Klasson (Eds.), *Biotechnology for Fuels and Chemicals* (pp. 763-774). Springer. https://doi.org/10.1007/978-1-60327-526-2_70

Kuo, C. H., Huang, C. Y., Shieh, C. J., Wang, H. M. D., & Tseng, C. Y. (2019). Hydrolysis of orange peel with cellulase and pectinase to produce bacterial cellulose using gluconacetobacter xylinus. *Waste and Biomass Valorization*, *10*, 85-93. https://doi.org/10.1007/s12649-017-0034-7

Leonarski, E., Cesca, K., Zanella, E., Stambuk, B. U., de Oliveira, D., & Poletto, P. (2021). Production of kombucha-like beverage and bacterial cellulose by acerola byproduct as raw material. *LWT*, *135*, Article 110075. https://doi.org/10.1016/j.lwt.2020.110075

Liang, J., Wang, R., & Chen, R. (2019). The impact of cross-linking mode on the physical and antimicrobial properties of a chitosan/bacterial cellulose composite. *Polymers*, *11*(3), Article 491. https://doi.org/10.3390/polym11030491

Lin, D., Liu, Z., Shen, R., Chen, S., & Yang, X. (2020). Bacterial cellulose in food industry: Current research and future prospects. *International Journal of Biological Macromolecules*, *158*, 1007-1019. https://doi.org/10.1016/j.ijbiomac.2020.04.230

Lin, W. C., Lien, C. C., Yeh, H. J., Yu, C. M., & Hsu, S. H. (2013). Bacterial cellulose and bacterial cellulose-chitosan membranes for wound dressing applications. *Carbohydrate Polymers*, *94*(1), 603-611. https://doi.org/10.1016/j.carbpol.2013.01.076

Malhotra, B., Keshwani, A., & Kharkwal, H. (2015). Antimicrobial food packaging: Potential and pitfalls. *Frontiers in Microbiology*, *6*, Article 611. https://doi.org/10.3389/fmicb.2015.00611

Oliveira, M. A., Gonzaga, M. L. C., Bastos, M. S. R., Magalhães, H. C. R., Benevides, S. D., Furtado, R. F., Zambelli, R. A., & Garruti, D. S. (2020). Packaging with cashew gum/gelatin/essential oil for bread: Release potential of the citral. *Food Packaging and Shelf Life*, *23*, Article 100431. https://doi.org/10.1016/j.fpsl.2019.100431

Revin, V., Liyaskina, E., Nazarkina, M., Bogatyreva, A., & Shchankin, M. (2018). Cost-effective production of bacterial cellulose using acidic food industry by-products. *Brazilian Journal of Microbiology*, *49*, 151-159. https://doi.org/10.1016/j.bjm.2017.12.012

Sharma, C., Bhardwaj, N. K., & Pathak, P. (2021). Static intermittent fed-batch production of bacterial nanocellulose from black tea and its modification using chitosan to develop antibacterial green packaging material. *Journal of Cleaner Production*, *279*, Article 123608. https://doi.org/10.1016/j.jclepro.2020.123608

Supian, N. N. I., Zakaria, J., Amin, K. N. M., Mohamad, S., & Sy Mohamad, S. F. (2021). Effect of fermentation period on bacterial cellulose production from oil palm frond (OPF) juice. *IOP Conference Series: Materials Science and Engineering*, *1092*, Article 012048. https://doi.org/10.1088/1757-899X/1092/1/012048

Szymańska, E., & Winnicka, K. (2015). Stability of chitosan-A challenge for pharmaceutical and biomedical applications. *Marine Drugs*, *13*(4), 1819-1846. https://doi.org/10.3390/md13041819

Tanpichai, S., Witayakran, S., Wootthikanokkhan, J., Srimarut, Y., Woraprayote, W., & Malila, Y. (2020). Mechanical and antibacterial properties of the chitosan coated cellulose paper for packaging applications: Effects of molecular weight types and concentrations of chitosan. *International Journal of Biological Macromolecules*, *155*, 1510-1519. https://doi.org/10.1016/j.ijbiomac.2019.11.128

Ul-Islam, M., Shah, N., Ha, J. H., & Park, J. K. (2011). Effect of chitosan penetration on physico-chemical and mechanical properties of bacterial cellulose. *Korean Journal of Chemical Engineering*, *28*, 1736-1743. https://doi.org/10.1007/s11814-011-0042-4

Wahid, F., Hu, X. H., Chu, L. Q., Jia, S. R., Xie, Y. Y., & Zhong, C. (2019). Development of bacterial cellulose/chitosan based semi-interpenetrating hydrogels with improved mechanical and antibacterial properties. *International Journal of Biological Macromolecules*, *122*, 380-387. https://doi.org/10.1016/j.ijbiomac.2018.10.105

Yusof, S. J. H. M., Roslan, A. M., Ibrahim, K. N., Abdullah, S. S. S., Zakaria, M. R., Hassan, M. A., & Shirai, Y. (2019). Life cycle assessment for bioethanol production from oil palm frond juice in an oil palm based biorefinery. *Sustainability*, *11*(24), Article 6928. https://doi.org/10.3390/SU11246928

Zahari, M. A. K. M., Ariffin, H., Mokhtar, M. N., Salihon, J., Shirai, Y., & Hassan, M. A. (2012). Factors affecting poly(3-hydroxybutyrate) production from oil palm frond juice by cupriavidus necator (CCUG52238 T). *Journal of Biomedicine and Biotechnology*, *2012*, Article 125856. https://doi.org/10.1155/2012/125865